ACADEMIC PRESS

Available online at www.sciencedirect.com

SCIENCE DIRECT®

Journal of Sound and Vibration 264 (2003) 135–155

JOURNAL OF SOUND AND VIBRATION

www.elsevier.com/locate/jsvi

# Transmission of fore–aft vibration to a car seat using field tests and laboratory simulation

Y. Qiu, M.J. Griffin*

*Human Factors Research Unit, Institute of Sound and Vibration Research, University of Southampton, Southampton SO17 1BJ, UK*

Received 30 November 2001; accepted 30 May 2002

**Abstract**

The transmission of fore–aft vibration to the seat cushion and backrest of a small car has been investigated by means of a field test and laboratory simulation methods. In the field test, transmissibilities to the seat backrest and the seat pan were computed using both single-input single-output and two-input one-output system models. The results showed that in the car the fore–aft vibration at the seat pan and the backrest depended not only on the fore–aft vibration of the floor but also on the vertical vibration of the floor. In the laboratory simulation, the transmissibilities were measured with 12 subjects and five different vibration stimuli. It was found that the fore–aft transmissibilities to both the backrest and the seat pan exhibited three resonance frequencies in the ranges 4–5, 25–30 and 45–50 Hz. The laboratory test also revealed that for the backrest and the seat pan, the resonance frequencies and the peak transmissibility at resonance changed with vibration magnitude, indicating non-linearity involving both seat–person systems. The field test and the laboratory test methods have different advantages. The correct vibration input spectra and the correct subject posture can be used in a field test, whereas a higher coherency can be obtained using the laboratory test. It was found that the low coherency in the field test when using the single-input and single-output assumption could be improved by adopting a two-input and one-output system model.


## 1. Introduction

Studies of the transmission of vertical vibration through the cushions of conventional seats have shown that there is usually amplification at low frequencies, often with a resonance at about 4 Hz, and attenuation only at frequencies greater than about 6 Hz [1]. Few studies have

*Corresponding author. Tel.: +44-23-8059-2277; fax: +44-23-8059-2927.
*E-mail address:* m.j.griffin@soton.ac.uk (M.J. Griffin).

0022-460X/03/$ - see front matter © 2002 Published by Elsevier Science Ltd.
doi:10.1016/S0022-460X(02)01171-9

investigated the transmission of fore–aft vibration through seat pan cushions, but some data suggest that in the fore–aft direction the transmission is close to unity over a wide range of frequencies [2,3].

The transmission of vibration to the backrest of a seat can also cause discomfort of drivers and passengers. In the vertical direction, the frequency weightings in current standards are such that vertical vibration of a backrest is unlikely to be a major contributor to discomfort unless there is a significant resonance in the backrest (see Refs. [4,5]). In the fore–aft direction, the frequency weightings suggest that if a cushion and backrest have the same level of vibration, the backrest will cause greater discomfort at frequencies greater than about 2 Hz. Any fore–aft resonance of the backrest will increase further the importance of backrest vibration to ride comfort. This high sensitivity to backrest vibration is the reason why evaluations of vehicle vibration often show the fore–aft vibration at the back as one of the three highest causes of discomfort in various forms of transport [6].

The measurement of fore–aft vibration on seat cushions and backrests can be affected by the angle of inclination of the surfaces: both the seat pan and the backrest are usually inclined rearwards. This inclination means that transducers used to measure vibration at the interfaces between a subject and a seat are not truly orientated in horizontal and vertical directions. The inclination of the transducers will result in them responding to a component of the vertical vibration on the seat pan or backrest: $\ddot{z}\sin\theta$, where $\ddot{z}$ is the vertical acceleration and $\theta$ is the angle of inclination. Even small angles (e.g., 10°) can result in significant levels of acceleration appearing in the 'fore–aft direction' due to the truly vertical vibration. In addition, the inclination of a backrest may result in fore–aft vibration due to the vertical vibration at the seat base. The causes of fore–aft vibration of a backrest may therefore be complex.

This study was conducted to investigate the transmission of fore–aft vibration through a car seat, recognizing that the vibration on the seat back measured in a car may arise from non-vertical vibration in the vehicle. The study was conducted in a car, with realistic vibration, and also in a laboratory where the input conditions could be controlled.

## 2. Car tests

### 2.1. Vibration measurement method

Measurements were made with a small family car that was driven over two different roads with two male subjects as drivers [7]. The car (Ford Focus, Zetec, 2.0 l) had a mass of 1300 kg and a wheelbase of 2615 mm. The weights and heights of the two subjects were 70 and 80 kg, and 170 and 183 cm, respectively. The seat consisted of a backrest (reclined at 15° to the vertical) and a seat pan (inclined at 12° to the horizontal). The seat pan and the backrest contained polyurethane foam (Fig. 1). The backrest frame was secured to the seat frame such that its angle could be adjusted by rotating a knob operating through a geared mechanism. The results presented here are for one driver on one road (with an unweighted fore–aft acceleration of 0.18 m s$^{-2}$ r.m.s.); similar results were obtained with this driver on the other road and with the second driver on both roads. During the measurements, the car was in fourth gear and moving at a constant 40 mile h$^{-1}$.

Fig. 1. Test seat from the car.

A total of nine channels of acceleration (fore–aft, lateral and vertical directions on the seat pan, backrest and floor) were recorded. Two 'SAE pads' conforming to ISO 10326-1 with built-in tri-axial accelerometers were positioned at the seat pan and the backrest as shown in Fig. 2. For measuring floor vibration, three piezoresistive accelerometers were mounted on a cube (orientated in the $x$, $y$ and $z$ directions) and fixed at the front left seat rail of the right-hand drive vehicle. The accelerometers were Entran model EGCS-DO-10/V10/L4M at the floor and Entran model EGCS-DO*-10V in the SAE pads.

The signals from the accelerometers were acquired to an HVLab data acquisition and analysis system (version 3.81). The measurement duration was 60 s and acceleration was sampled at 200 samples/s via 67 Hz anti-aliasing filters. Frequency analysis was performed using an actual frequency resolution of 0.78 Hz with 188 degrees of freedom.

The power spectral density (PSD) functions computed from fore–aft acceleration time histories from the conditions mentioned above are shown in Fig. 3. The results show how the fore–aft

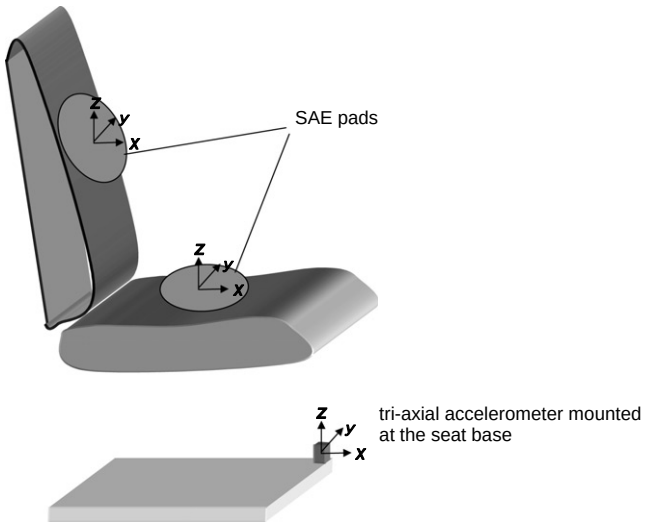


Fig. 2. Installation of SAE pads and accelerometers on the seat.

vibration acceleration at the floor, backrest and seat pan were distributed over the frequency range up to 50 Hz. A peak was consistently found around 20 Hz for both floor and seat pan fore–aft vibration; backrest fore–aft vibration acceleration was mostly in the range below 10 Hz.

Seat transmissibility was initially determined using a single-input and single-output assumption. A two-input and one-output model was then introduced to investigate the transmissibility induced by both fore–aft and vertical vibration at the seat base (i.e., the floor).

### 2.2. Seat transmissibility from single-input and single-output model

From single-input and single-output linear system theory, the transfer function and the ordinary coherency (in the range 0–1) between the input signal $x(t)$ and the output signal $y(t)$ are computed as

$$H(f) = \frac{G_{xy}(f)}{G_{xx}(f)}$$

and

$$\gamma_{xy}^2(f) = \frac{|G_{xy}(f)|^2}{G_{xx}(f)G_{yy}(f)}.$$

In the above equations, $G_{xx}(f)$ and $G_{yy}(f)$ represent the power spectral density functions of $x(t)$ and $y(t)$, respectively, and $G_{xy}(f)$ is the cross-spectral density function between the two signals. The seat transmissibilities and corresponding coherencies were computed from the floor acceleration in one axis ($\ddot{x}_f$, $\ddot{y}_f$ or $\ddot{z}_f$, where double dot indicates acceleration) and the seat or backrest acceleration in the same direction. The results for fore–aft vibration are shown in Fig. 4. As can be seen, the transmissibility from the floor to the backrest exhibits two peaks, one located around 4–5 Hz and the other between 28 and 30 Hz, whereas the transmissibility from the floor to the seat pan shows two distinctive resonance frequencies, around 2 and 28 Hz.

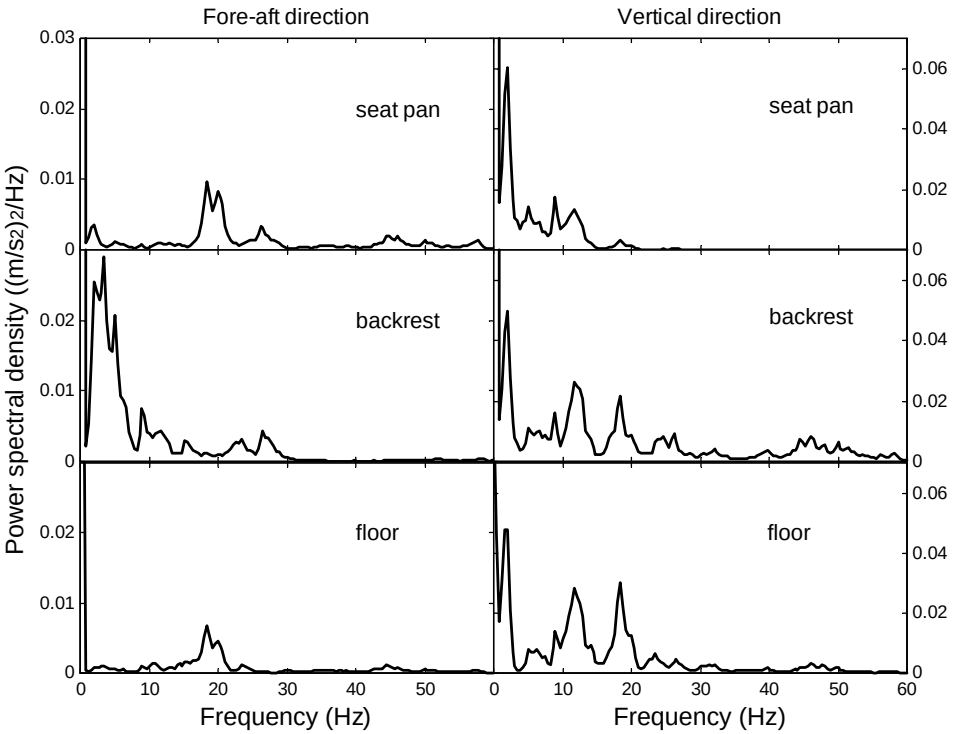


Fig. 3. Power spectral densities in the fore–aft and vertical directions measured from the seat pan, the backrest and the seat base (floor) in the car (0.78 Hz resolution, 188 degrees of freedom).

In Fig. 4, and for the transmissibilities computed from the lateral and vertical accelerations (not shown), the coherencies are poor. For vertical vibration, it may sometimes be reasonable to assume a seat is a single-input and single-output system and compute the ordinary coherence function when the frequency range is below 20 Hz, as a coherence of 0.8 or more can often be reached over this frequency range [6]. For fore–aft vibration, a low coherence was observed when using the single-input model, as can be seen in Fig. 4. The single-input and single-output assumption seems insufficient. Fore–aft vibration on the seat pan and the backrest might be induced not only by the fore–aft vibration on the floor but also by the vertical vibration on the floor (partly due to the inclination of the seat pan and the backrest), and possibly by pitch motion of the vehicle. A more complete approach to the determination of seat transfer functions in the fore–aft direction is to consider the seat as a two-input and one-output system or, in general, a multiple-input and multiple-output system.

### 2.3. *Seat transmissibility from two-input and one-output model*

#### 2.3.1. *Brief description of the model*

A system with two inputs, $x_1(t)$ and $x_2(t)$, and one output, $y(t)$, is shown in Fig. 5. In the case that the noise term $n(t)$ is uncorrelated with $x_1(t)$ and $x_2(t)$, the output power spectral density can

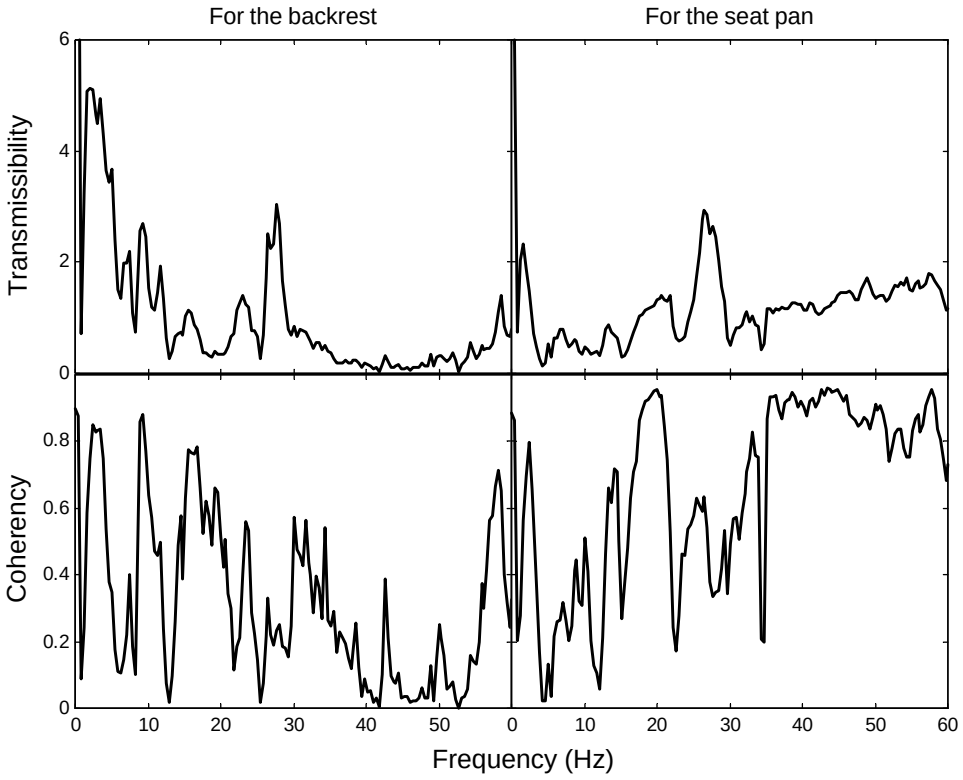


Fig. 4. Transmissibility and coherency from single-input and single-output model in the field test (0.78 Hz resolution, 188 degrees of freedom).

be calculated as [8]

$$G_{yy}(f) = |H_{1y}(f)|^2 G_{11}(f) + H_{1y}^*(f) H_{2y}(f) G_{12}(f) + H_{2y}^*(f) H_{1y}(f) G_{21}(f) + |H_{2y}(f)|^2 G_{22}(f) + G_{nn}.$$

The transfer functions for the original system, $H_{1y}(f)$ and $H_{2y}(f)$, can be computed as

$$H_{1y}(f) = \frac{G_{1y}(f)[1 - (G_{12}(f)G_{2y}(f)/G_{22}(f)G_{1y}(f))]}{G_{11}(f)[1 - \gamma_{12}^2(f)]},$$

$$H_{2y}(f) = \frac{G_{2y}(f)\left[1 - (G_{21}(f)G_{1y}(f)/G_{11}(f)G_{2y}(f))\right]}{G_{22}(f)[1 - \gamma_{12}^2(f)]}.$$

In the above equations, $G_{11}$, $G_{22}$ and $G_{12} = G_{21}^*$ (where * represents the complex conjugate) are the power spectral density functions of $x_1(t)$ and $x_2(t)$ and the cross-spectral density function between $x_1(t)$ and $x_2(t)$, respectively. $G_{1y}$ and $G_{2y}$ represent the cross-spectral density functions between $x_1(t)$ and $y(t)$ and between $x_2(t)$ and $y(t)$, and $\gamma_{12}^2$ is the ordinary coherency between $x_1(t)$ and $x_2(t)$. To show how well the two inputs together linearly account for the measured output, the multiple

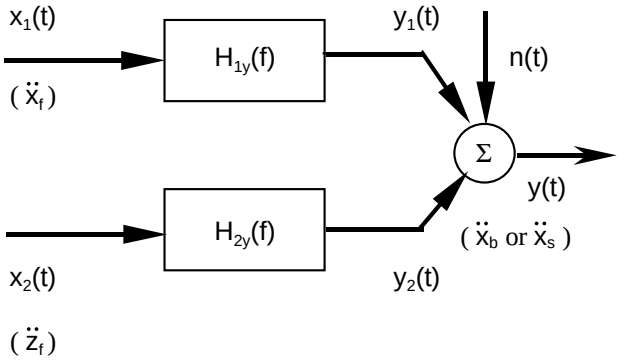


Fig. 5. Block diagram for original two-input and one-output system.

coherence function can be computed as

$$\gamma^2_{y:x}(f) = \frac{G_{vv}(f)}{G_{yy}(f)},$$

where $G_{vv}(f)$ represents the ideal output spectrum due to the two inputs. It can be computed as

$$G_{vv}(f) = G_{yy}(f) - G_{nn}(f).$$

Furthermore, to identify how much one of the inputs alone linearly accounts for the measured output, partial coherence functions can be calculated. To this end, the so-called conditioned two-input and one-output system needs to be determined. To proceed with signal processing, it is assumed that $x_1(t)$ should precede $x_2(t)$ and any correlation between $x_1(t)$ and $x_2(t)$ comes from $x_1(t)$, the original signal $x_2(t)$ can be decomposed into two parts:

$$x_2(t) = x_{2:1}(t) + x_{2.1}(t)$$

with $x_{2:1}(t)$ representing the linear effect of $x_1(t)$ to $x_2(t)$ and the conditioned signal, $x_{2.1}(t)$, being that part of $x_2(t)$ not due to $x_1(t)$. After this treatment, the original system in Fig. 5 is equivalent to the conditioned system shown in Fig. 6. Since the inputs are now mutually uncorrelated, the system is equivalent to two separate single-input and single-output models. In other words, $L_{1y}$ is the optimum system to predict $y$ from input $x_1$, whereas $L_{2y}$ is the optimum system to predict $y$ from conditioned input $x_{2.1}$. The transfer functions of the optimum system for the conditioned inputs can be computed as

$$L_{1y}(f) = \frac{G_{1y}(f)}{G_{11}(f)}, \quad L_{2y}(f) = \frac{G_{2y.1}(f)}{G_{22.1}(f)},$$

where $G_{2y.1}(f)$ is the cross-spectral density function between the conditioned input $x_{2.1}(t)$ and output $y(t)$, and $G_{22.1}(f)$ is conditioned autospectrum of $x_{2.1}(t)$. They are computed as

$$G_{2y.1}(f) = G_{2y}(f) - \left[\frac{G_{21}(f)}{G_{11}(f)}\right] G_{1y}(f), \quad G_{22.1}(f) = [1 - \gamma^2_{12}(f)]G_{22}(f).$$

Since the output terms $v_1(t)$, $v_2(t)$ and $n(t)$ in Fig. 7 are mutually uncorrelated, the measured output autospectrum $G_{yy}(f)$ is simply the sum of three autospectra terms with no cross-spectra

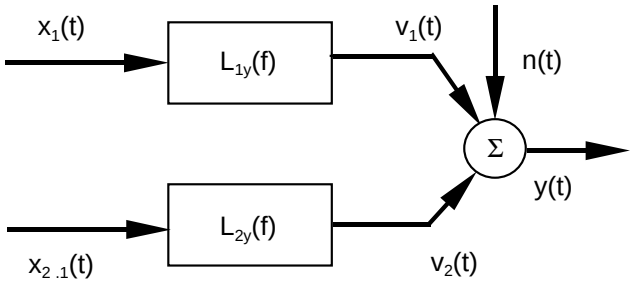


Fig. 6. Block diagram for conditioned two-input and one-output system.

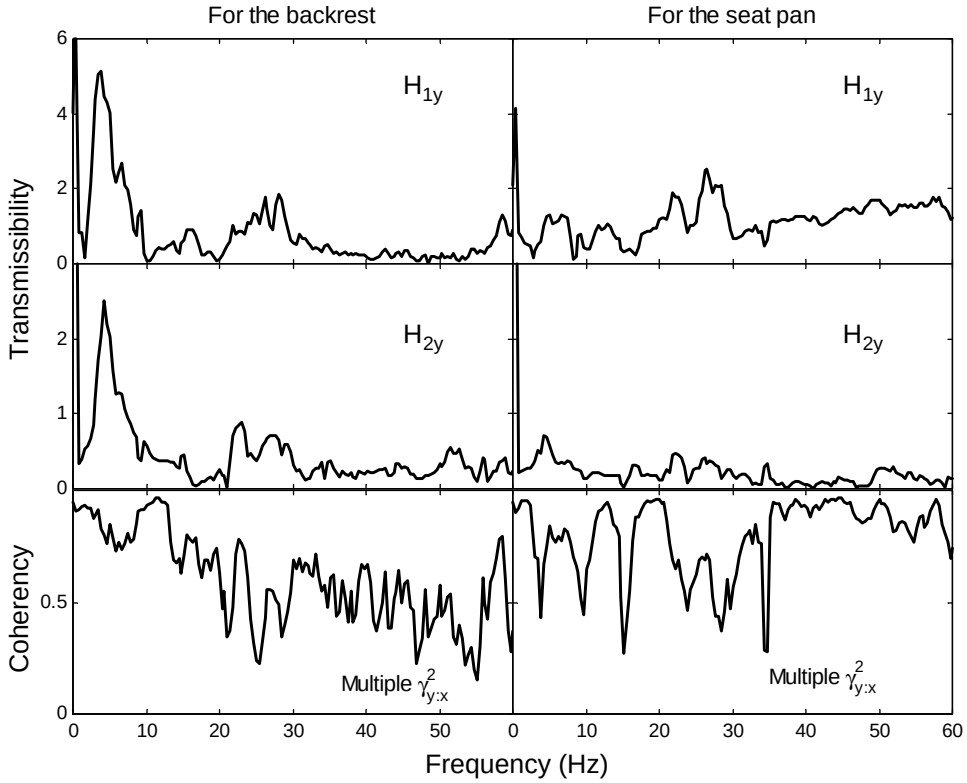


Fig. 7. Transfer function for original inputs and multiple coherency from two-input and one-output model in the field test (0.78 Hz resolution, 188 degrees of freedom), $H_{1y}$ and $H_{2y}$ are transfer functions to the output from original inputs 1 and 2, respectively.

terms, that is,

$$G_{yy}(f) = G_{v_1v_1}(f) + G_{v_2v_2}(f) + G_{nn}(f).$$

Hence, the ordinary coherence function between $x_1(t)$ and $y(t)$ is computed as

$$\gamma_{1y}^2(f) = \frac{G_{v_1v_1}(f)}{G_{yy}(f)} = \frac{|G_{1y}(f)|^2}{G_{11}(f)G_{yy}(f)}.$$

The partial coherence function between the conditioned signals $x_{2.1}(t)$ and $yy._1(t)$ (which represents part of the output term $y(t)$ not due to $x_1(t)$) is defined by

$$\gamma^2_{2y.1}(f) = \frac{G_{v_2v_2}(f)}{G_{yy}(f)} = \frac{|G_{2y.1}(f)|^2}{G_{22.1}(f)G_{yy.1}(f)}.$$

*2.3.2. Computational results*

Choosing fore–aft vibration at the car floor, $\ddot{x}_f$, as input $x_1(t)$ and floor vertical vibration, $\ddot{z}_f$, as input $x_2(t)$, the transfer functions for the original and conditioned systems and the multiple and partial coherencies for the seat pan and the backrest were evaluated.

The optimum systems for the original inputs, $H_{1y}(f)$ and $H_{2y}(f)$, accounting for the fore–aft vibration transmission from two mutually correlated inputs ($\ddot{x}_f$ and $\ddot{z}_f$) to the backrest ($\ddot{x}_b$), and the results corresponding to the seat pan are shown in Fig. 7. It is interesting to see that the floor vertical acceleration ($\ddot{z}_f$) makes a significant contribution to the backrest acceleration in the fore–aft direction. The transmissibilities $H_{1y}(f)$ and $H_{2y}(f)$ in the case of the backrest exhibit two resonance frequencies (around 4 and 28 Hz). In the case of the seat pan, two resonances (around 5 and 25 Hz) were found associated with the transfer function of the original system. The multiple coherence functions for both the backrest and the seat pan are also shown in Fig. 7 which show how well the two inputs together linearly account for the measured output.

The optimum systems for the conditioned inputs, $L_{1y}$ and $L_{2y}$, accounting for the vibration of the backrest and the seat pan (output) in the fore–aft direction separately from input $\ddot{x}_f$ and conditioned input $\ddot{z}_f$ are shown in Fig. 8, together with the corresponding ordinary and partial coherencies. With respect to the resonance frequency, features similar to those observed in $H_{1y}(f)$ and $H_{2y}(f)$ can be seen. It should be recognized that, in the order the two inputs were defined in the model ($\ddot{x}_f$ as input 1 and $\ddot{z}_f$ as input 2), the ordinary coherency in Fig. 8 indicates how much of the first input $\ddot{x}_f$ is linearly related to the output ($\ddot{x}_b$ or $\ddot{x}_s$), whereas the partial coherency reflects contributions to the output from the second input $\ddot{z}_f$ (after signal conditioning). From Fig. 8, it is seen that, for both cases of the backrest and the seat pan, the ordinary and partial coherencies display a reasonably strong coherence of 0.5–0.9 over some parts of the frequency range. This indicates that both the fore–aft acceleration and the vertical acceleration at the floor contributed to the fore–aft motion of the backrest and the seat pan. Inspection of the ordinary and partial coherencies reveals that both inputs (floor fore–aft acceleration, $\ddot{x}_f$, and the conditioned vertical acceleration, $\ddot{z}_f$) exhibited nearly equal effects on the fore–aft vibration of the backrest. On the other hand, the fore–aft motion of the seat pan seems to be more correlated with the fore–aft acceleration at the floor ($\ddot{x}_f$) than the vertical acceleration at the floor ($\ddot{z}_f$). It is evident from Fig. 8 that, for the seat pan, the ordinary coherency is, overall, greater than the partial coherency, especially in high frequency range ($>15$ Hz) where a stronger coherence was found in the ordinary coherence function between input $\ddot{x}_f$ and output $\ddot{x}_s$ than in the partial coherence function between conditioned input $\ddot{z}_f$ and the output. It may also be noted that the partial coherency between the fore–aft acceleration at the seat pan and the conditioned vertical acceleration at the floor is slightly lower than the backrest (Fig. 8). This may be because the inclination of the seat pan is less than that of the backrest.

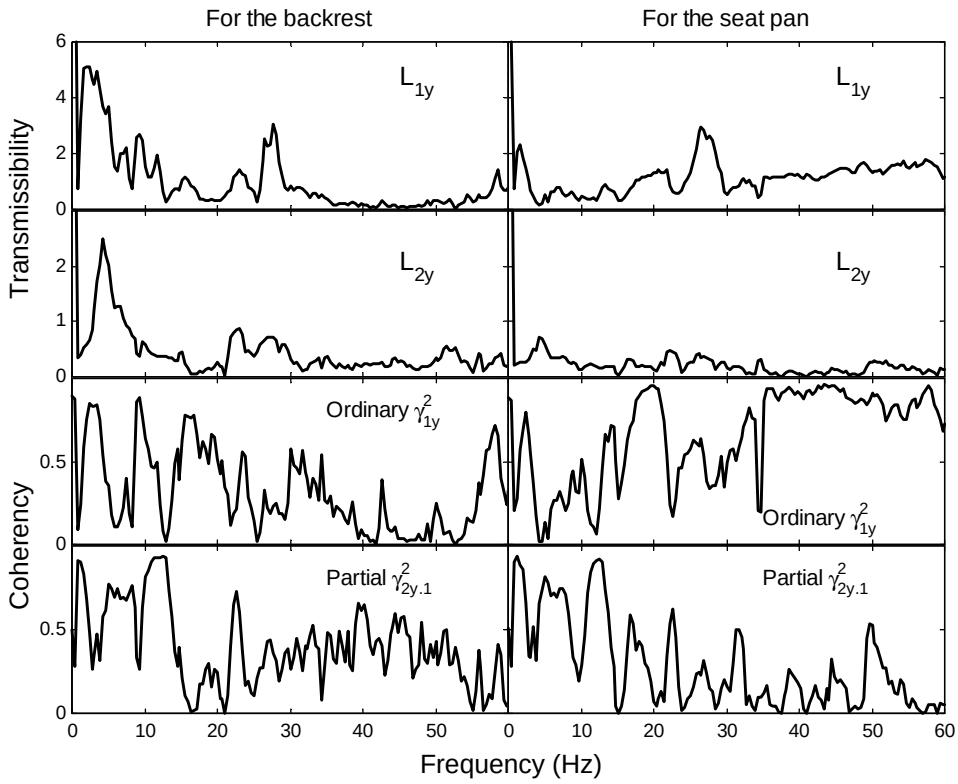


Fig. 8. Transfer function for conditioned inputs and ordinary and partial coherency from two-input and one-output model in the field test (0.78 Hz resolution, 188 degrees of freedom), $L_{1y}$ and $L_{2y}$ are transfer functions to the output from conditioned inputs 1 and 2, respectively.

### 2.4. Discussion

Comparing the transmissibility results from the single-input single-output model with those from the two-input one-output model, it can be seen that the characteristics of the transmissibilities from both systems are similar. Nevertheless, comparing values of the coherence functions from the two systems over the frequency range 0–60 Hz, a higher coherency was observed after taking into consideration the effect of the floor vertical vibration. This can be seen in Fig. 9, which shows the ordinary coherencies for the backrest and the seat pan computed from the single-input and single-output model compared with their multiple coherencies from a two-input and one-output model. It is clear that fore–aft motion on the backrest was not only caused by fore–aft vibration on the floor. The vertical vibration on the seat base also had a significant influence on the vibration transmission to the backrest. This was also true for the seat pan.

The results show that a single-input and single-output model is not sufficient to study vibration transmission to a vehicle seat in the fore–aft direction. Consider, as an example, the transmission of fore–aft and vertical vibration from the seat base to fore–aft motion of the backrest via the two-input model, as shown in Fig. 6 where $x_1$, $x_{2.1}$ and $y$ are replaced by $\ddot{x}_f$, $\ddot{z}_f$ (after conditioning) and

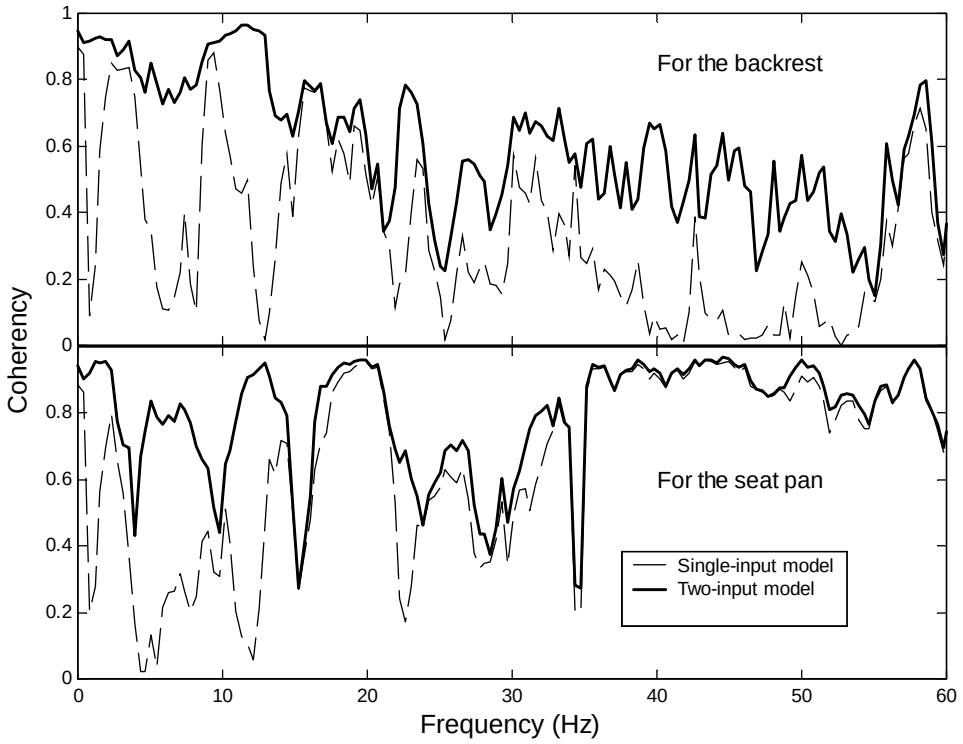


Fig. 9. Comparison of ordinary coherency from single-input and single-output model to multiple coherency from two-input and one-output model, for the backrest and the seat pan (0.78 Hz resolution, 188 degrees of freedom), field test.

$\ddot{x}_b$, respectively. Fig. 10 shows power spectral densities of different signals $v_1(t)$, $v_2(t)$ and $y(t)$ and the summation of the power spectra of $v_1(t)$ and $v_2(t)$ with reference to Fig. 6. Inspection of the spectra $Gv_1$ (in dotted line, due to $\ddot{x}_f$) and $Gv_2$ (in dashed line, due to conditioned $\ddot{z}_f$) shows that both fore–aft and vertical vibration at the seat base contributed to the vibration of the seat backrest. The spectrum $Gv_1$ is the same as the counterpart from a single-input model with $\ddot{x}_f$ as input and $\ddot{x}_b$ as output. There exists a distinct discrepancy between $Gv_1$ (for the single-input model) and the total output energy $Gx_b$ (in thick solid line), indicating some important input signal was missing. On the other hand, for the two-input model, the summation of $Gv_1$ and $Gv_2$ (in thin solid line) is much closer to $Gx_b$, as can be seen in Fig. 10, indicating the second input has played an important role. Consider the seat transmissibility curves $L_{1y}$ and $L_{2y}$ for the backrest (top two curves in the left column of Fig. 8) computed using the two-input model. The transmissibility from the fore–aft motion of the seat base to the fore–aft motion of the backrest ($L_{1y}$) is the same as that from the single-input model (Fig. 4 in the top left-hand corner). Nevertheless, the transmissibility from the vertical motion of the seat base (conditioned) to the fore–aft motion of the backrest ($L_{2y}$) has substantial values (i.e., 1.0–2.5) over the frequency range 3–7 Hz and exhibit a non-negligible effect. Clearly, the single-input model failed to include the effect of the vertical vibration at the seat base, which was substantial.

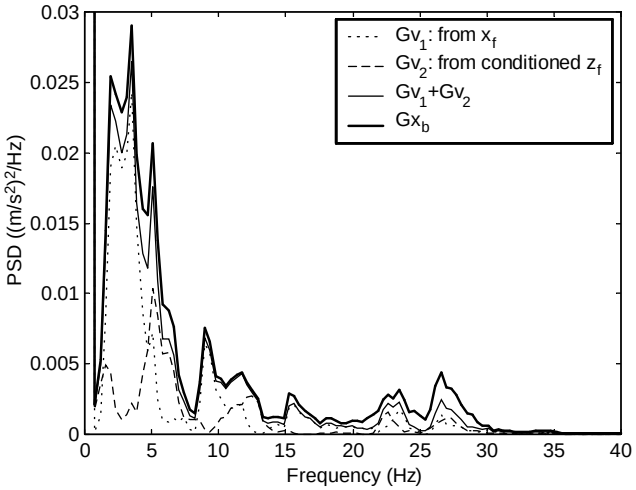


Fig. 10. Power spectral densities with two-input (fore–aft, $\ddot{x}_f$, and vertical, conditioned $\ddot{z}_f$, vibration at the seat base) and one-output (fore–aft motion, $\ddot{x}_b$, at the backrest) model in relation to Fig. 6. $Gv_1$ is the power spectral density at the output end of the first path due to $\ddot{x}_f$, which is the same as its counterpart in a single-input and single-output model. $Gv_2$ is the power spectral density at the output end of the second path due to conditioned $\ddot{z}_f$. $Gx_b$ is the measured power spectral density of the fore–aft motion at the seat backrest.

A vehicle seat is therefore a multi-input vibration system. A full understanding of vibration transmission in a vehicle seat requires the computation of partial coherence functions. Using a two-input or a multi-input model, the effect of two or more input sources on the seat transmissibility can be investigated. It has been demonstrated that a two-input and one-output model is a more reasonable assumption to study the transmission of fore–aft vibration from the seat base to the backrest and the seat pan.

To further investigate the transmission of fore–aft vibration through the seat, a laboratory experiment was conducted.

## 3. Measurement of fore–aft seat transmissibility in laboratory

### *3.1. Experimental conditions*

Twelve subjects (9 males and 3 females) aged from 20 to 55 years participated in a laboratory experiment using a 1-m stroke horizontal simulator within the laboratories of the Human Factors Research Unit at the Institute of Sound and Vibration Research in the University of Southampton. The experiment was approved by the Human Experimentation, Safety and Ethics Committee of the Institute.

The same seat used in the car field test described above was secured to the vibrator that was excited with three random acceleration time histories having flat constant bandwidth spectra over the frequency range 0.4–60 Hz and presented at three magnitudes (0.498, 1.015 and 1.951 $\mathrm{m\,s^{-2}}$ r.m.s.). In addition, the seat was excited by two fore–aft acceleration time histories

recorded on the floor during the road test and filtered to contain only frequency components in the range 0.4–60 Hz and presented with overall magnitudes of 0.18 and 0.20 m s$^{-2}$ r.m.s. The recorded time histories were compensated for the response of the simulation system so that the measured errors between the desired signals and the motion achieved on the simulator table, in terms of magnitude of acceleration r.m.s values, were within a range of 0.4–3.8%. The *relative error* as a function of frequency was investigated using power spectral densities and was computed as

$$\textit{relative error} = \frac{|G'_x - G_x|}{Gx} \times 100,$$

where $G'_x$ and $G_x$ are the power spectral density functions from the real signal and the desired signal. The obtained relative error in the power spectral densities was less than about 20% at frequencies where there was significant motion.

During the experiment, each subject was exposed to the same five stimuli. Each exposure lasted 60 s with a sampling rate of 200 samples/s. Five channels of acceleration were recorded: the fore–aft acceleration of the simulator table, the fore–aft acceleration of the seat pan surface and the backrest, and vertical acceleration of the seat pan surface and the backrest.

The signals were generated, and the transmissibilities and coherence functions were calculated, using *HVLab* data acquisition and signal processing package (version 3.81). The actual resolution was 0.39 Hz and the degrees of freedom were 96. Figs. 11–13 show the transmissibilities and coherencies measured from the 12 subjects for two of the input motions: a random stimulus (1.015 m s$^{-2}$ r.m.s.) and a road test signal input (0.18 m s$^{-2}$ r.m.s.). The transmissibility and coherence functions shown were computed using a single-input and single-output model, as the input source on the simulator only contained motion in the fore–aft direction.

### 3.2. Results and discussion

#### 3.2.1. Transmissibility from the floor to the backrest

Fig. 11 shows the fore–aft transmissibility and coherency to the backrest for all 12 subjects exposed to the 1.015 m s$^{-2}$ r.m.s. random vibration. The transmissibility exhibits three resonance frequencies: at about 5 Hz, around 28 Hz and at about 48 Hz. For about 40% of the subjects, the transmissibility presents only one distinctive resonance frequency (at about 5 Hz). From Fig. 11 it can be seen that a strong coherence of 0.8–0.98 was observed for most of the 12 subjects. For one measurement (at about 28 Hz for one subject), the coherency dropped to below 0.1, and the corresponding transmissibility dropped to nearly zero, as can be seen in the figure. The diminishing coherence at this frequency (28 Hz) for this individual probably resulted from contributions of extraneous measurement noise or caused by an inadvertent posture change during the experiment. Indeed, at this frequency the transmissibility for this subject was so low that the acceleration measured on the seat was primarily noise.

Fig. 12 shows data similar to Fig. 11 but for the road vibration input. The coherency with the road input signal was poorer than with the broad-band random input signal, presumably because the input magnitude was lower and the input energy was not equally distributed over the spectrum.

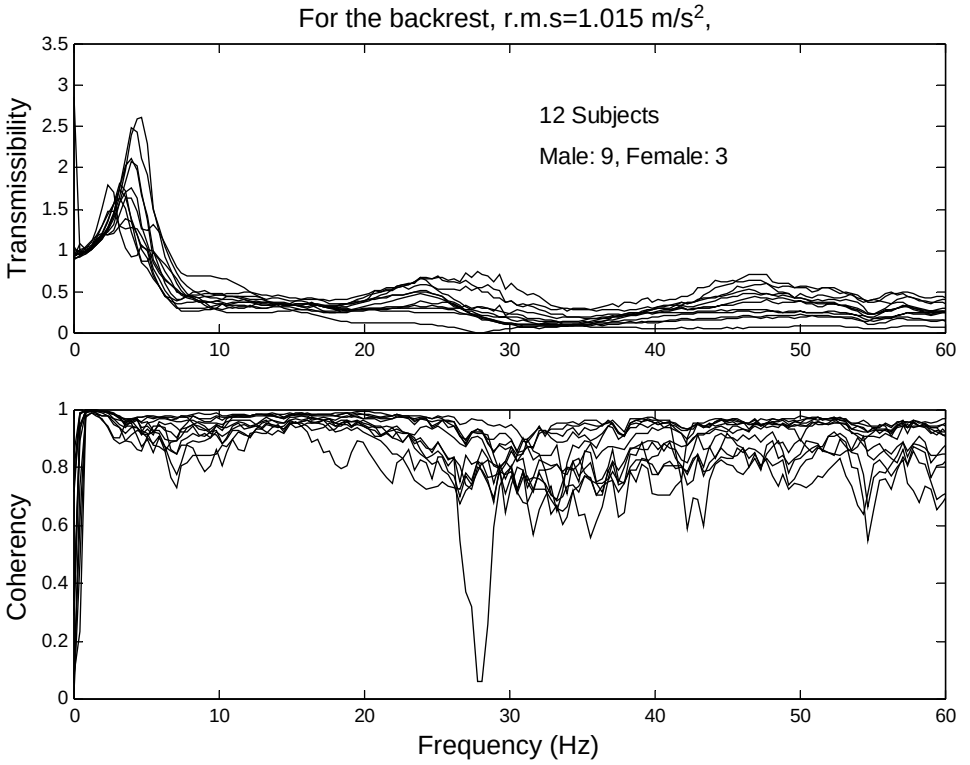


Fig. 11. Transmissibility and coherency of the backrest in fore–aft direction (0.39 Hz resolution, 96 degrees of freedom), random vibration input with acceleration r.m.s value = 1.015 m s$^{-2}$, laboratory simulation.

Fig. 13 compares the median fore–aft transmissibilities of the seat backrest with the 12 subjects using three vibration magnitudes (random signals at 0.498, 1.015 and 1.951 m s$^{-2}$ r.m.s). The results show that, while the primary resonance frequency changed only a little, the primary peak in the transmissibility decreased with increasing vibration magnitude, indicating a non-linearity in the backrest–person system. This has been supported by a statistical test in which the significance of changes of the primary resonance frequency and the corresponding peak value of transmissibility with magnitude were investigated using the Friedman two-way analysis of variance by ranks test [9] based on the data from the 12 subjects. It was found that, while the change in the resonance frequency with vibration magnitude was only marginally significant ($p = 0.061$), the change in the peak transmissibility with vibration magnitude was highly significant ($p < 0.001$). For the second mode of vibration (Fig. 13), it appears that both the peak of the transmissibility and the resonance frequency decreased with increasing vibration magnitude (suggesting a non-linear softening system). However, the statistical test indicated that while the change of the resonance frequency with magnitude was highly significant ($p < 0.001$), the influence of vibration magnitude on the peak transmissibility was not statistically significant ($p = 0.174$). It appears that the non-linear phenomenon associated with the second mode might be attributed to non-linear stiffness of the backrest–person system. For the third mode of vibration, no consistent change to the resonance was seen with changing vibration magnitude.

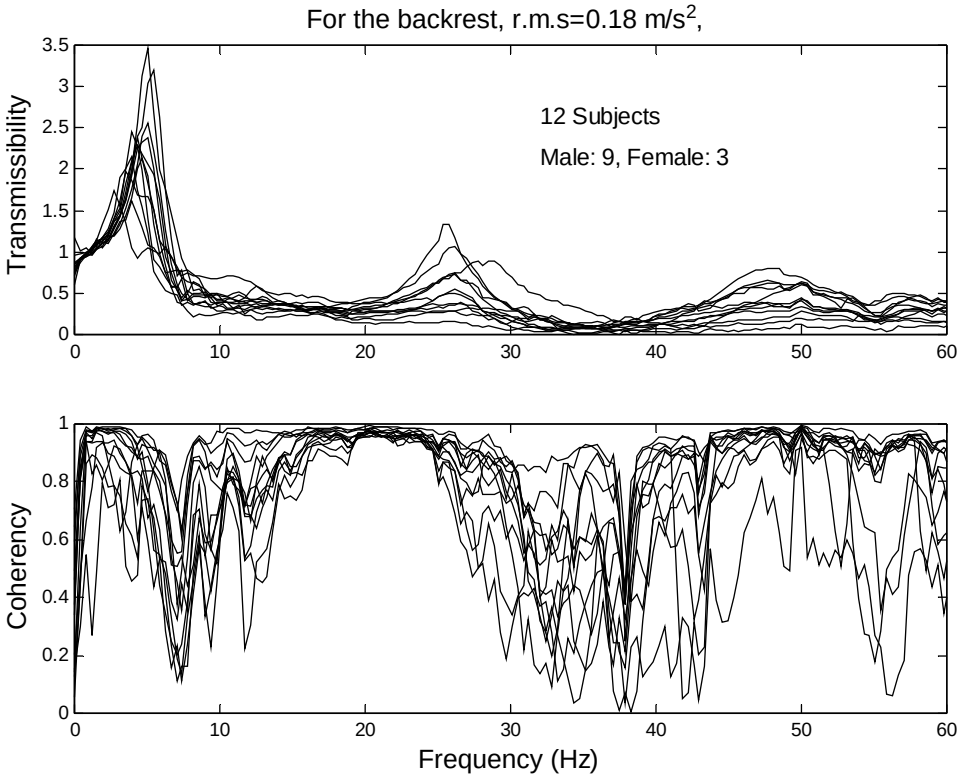


Fig. 12. Transmissibility and coherency of the backrest in fore–aft direction (0.39 Hz resolution, 96 degrees of freedom), road vibration input with acceleration r.m.s value = 0.18 m s$^{-2}$, laboratory simulation.

### 3.2.2. *Transmissibility from the floor to the seat pan*

The fore–aft transmissibilities of the seat pan and the corresponding coherence functions obtained with the random vibration input are presented in Fig. 14. Similar to the backrest, the seat–person system presented three resonance frequencies over the range 0–60 Hz, with a distinctive resonance located at about 5 Hz. Although the peaks are not as obvious as with the backrest, the three resonance frequencies were located at about the same positions as those for the backrest. The coherency for the fore–aft transmissibility of the seat is much higher than that for the backrest. In other words, the fore–aft vibration of the seat base was more closely related to the fore–aft motion of the seat pan than to that of the backrest. One reason may be that the shear transmissibility of the seat pan is more rigid than the compressive transmissibility of the backrest and, in addition, the seat surface has less inclination than the backrest.

Fig. 15 shows the seat transmissibility and coherency in the fore–aft direction when using the road signal as the input. The results appear to be consistent with those presented in Fig. 14. It is interesting to notice from Figs. 14 and 15 that the scatter in the seat pan transmissibilities over the 12 subjects is less at frequencies below 25 Hz than at higher frequencies. It appears that the first two resonance frequencies were consistent for all 12 subjects. The third resonance, however,

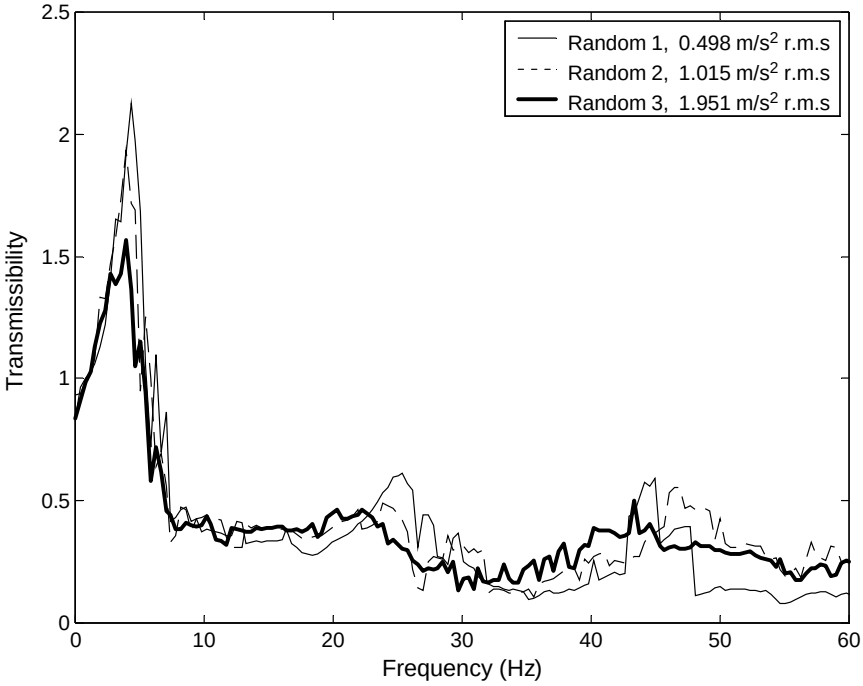


Fig. 13. Median transmissibility of the backrest from 12 subjects and three random vibration inputs (acceleration r.m.s. values = 0.498, 1.015 and 1.951 $m\,s^{-2}$), laboratory simulation.

varied remarkably from person to person and no consistent resonance can be found at frequencies greater than 25 Hz.

The effect of vibration magnitude on the median transmissibility of the seat pan is shown in Fig. 16. At both the first and the second modes of vibration, the resonance frequencies decreased with increasing vibration magnitude. Similar to the backrest, the peak of the transmissibility at the first mode decreased with increasing vibration magnitude. However, at the second resonance and at higher frequencies, the transmissibility increased with increasing vibration magnitude. The statistical test for the first three modes of vibration indicated that the changes of all three resonance frequencies and the corresponding peaks of transmissibilities with magnitude were statistically significant for both resonance frequency and peak transmissibility ($p < 0.003$).

### 3.3. Comparison with field test

Although the trends in the transmissibility and resonance frequency from the two methods are similar, there are differences between the transmissibilities measured in the field test and those from the laboratory simulation. Fig. 17 compares the transmissibility and coherency of the backrest and the seat pan between the field test and the laboratory simulation (both were computed using a single-input and single-output model) for the same individual subject. It can be seen from Fig. 17 that the coherency from the laboratory simulation is much higher than that from the field test, whereas the transmissibility from the field test is generally

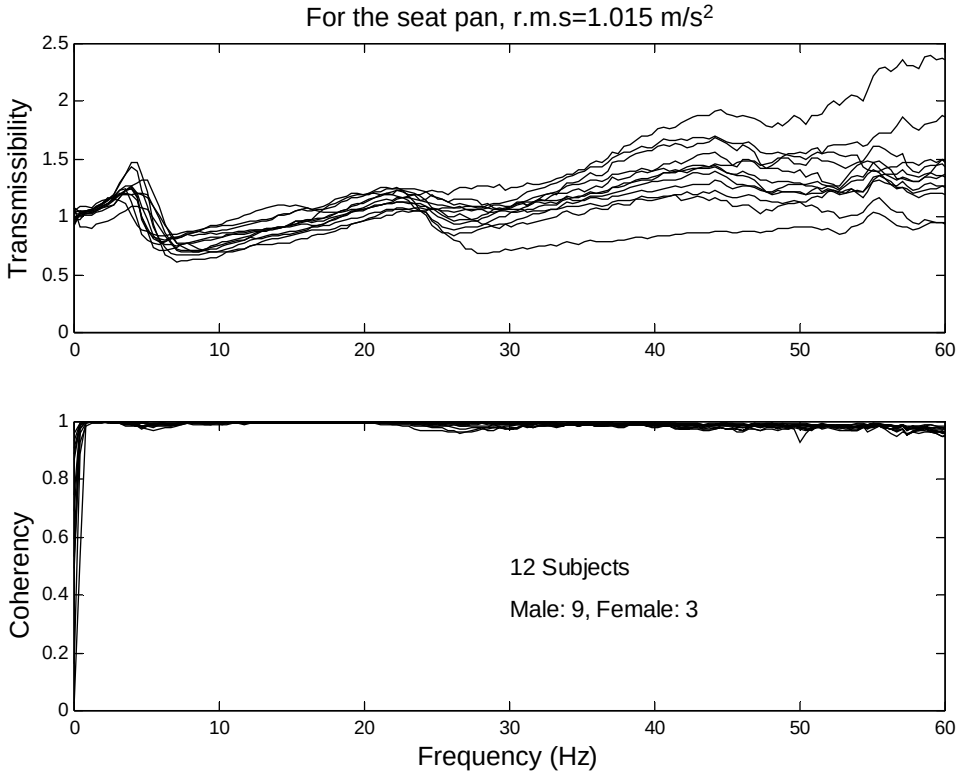


Fig. 14. Transmissibility and coherency of the seat pan in fore–aft direction (0.39 Hz resolution, 96 degrees of freedom), random vibration input with acceleration r.m.s value = 1.015 m s$^{-2}$, laboratory simulation.

greater than its counterpart from the laboratory test. The differences may have arisen for several reasons.

In the laboratory test, the input only contained vibration in one direction (fore–aft), whereas in the field test, the input came from several sources: the fore–aft vibration of the seat base, the vertical vibration of the base and even pitch or roll motion of the vehicle. The reason for the seat transmissibility from the field test being in general greater than that from the laboratory test is partly because among several possible input sources only the fore–aft vibration was considered when computing the transmissibility for the field test. The increased transmissibility in the field test is not so obvious for the seat pan as for the backrest (Fig. 17, right side). This may be because the effect of pitch and roll motions on the seat pan were not as significant as on the backrest, and the contribution of the vertical input to the seat pan is relatively small due to a smaller inclined angle of the seat pan than the backrest. Fig. 17 also shows that at some frequencies the transmissibility of the seat pan from the field test is slightly less than its counterpart from the laboratory test. This is because, for this particular test, the vibration transmission from fore–aft motion of the seat base to the fore–aft motion of the seat pan was observed to be out of phase from that caused by the vertical motion of the seat base.

In the field test, the input was quite low and did not contain sufficient energy to obtain a good coherency at all frequencies, whereas in the laboratory, input energy can be well defined over the

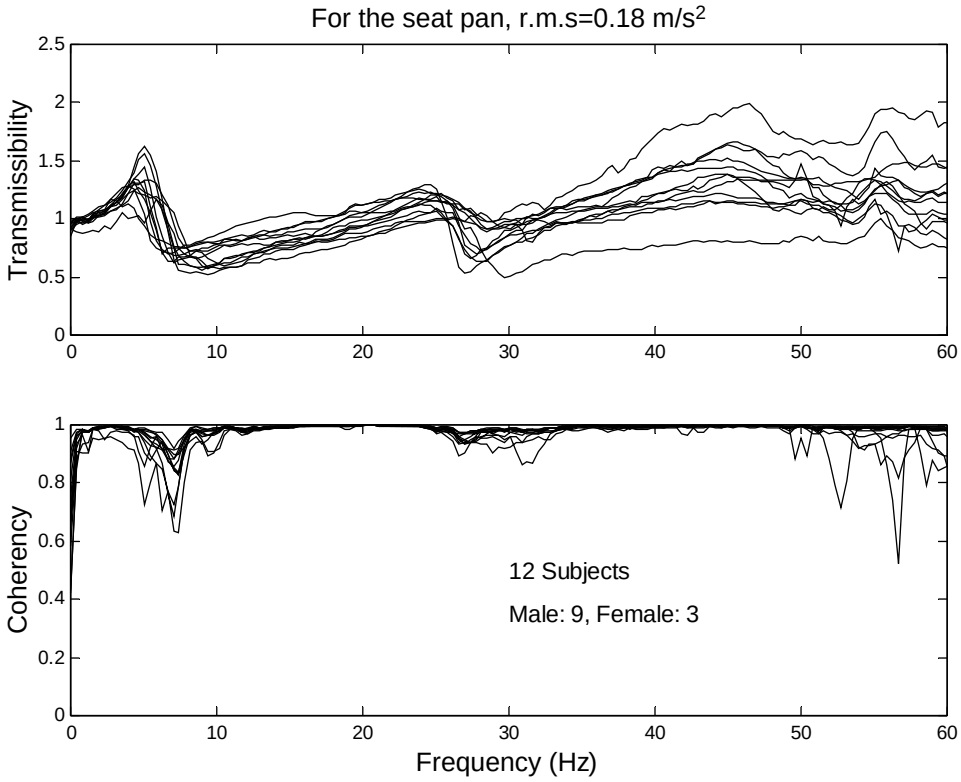


Fig. 15. Transmissibility and coherency of the seat pan in fore–aft direction (0.39 Hz resolution, 96 degrees of freedom), road vibration input with acceleration r.m.s value = 0.18 m s$^{-2}$, laboratory simulation.

whole frequency range of interest. However, even if the coherencies had been higher, the transmissibilities would not be expected to be the same if the input vibration used in the laboratory differed greatly from that in the field, because the dynamic response of the seat–person system is not linear.

Another possible cause of differences in the transmissibilities between the field test and laboratory simulation may be non-rigidity in the seat base. In the laboratory test, the support structure beneath the seat behaved as a rigid body but this may not have been the case in the vehicle. Non-rigidity of the seat base will require the use of a more complex multi-input model rather than the single-input and two-input models used here to compute seat transmissibility.

Because of the differences between the laboratory and the field tests, both have their advantages. With the field test, the correct multi-axis vibration input spectra and the correct subject posture can be used. It has been shown that the low coherency phenomenon encountered in the field test under single-input single-output assumption can be improved by adopting a two-input and one-output system model. When it is not possible to measure the response in the appropriate vehicle, laboratory measurements of seat transmissibility become necessary. A much better coherency can be obtained using the laboratory method than using the field test method. Since the input spectrum can be controlled, the laboratory method may determine the

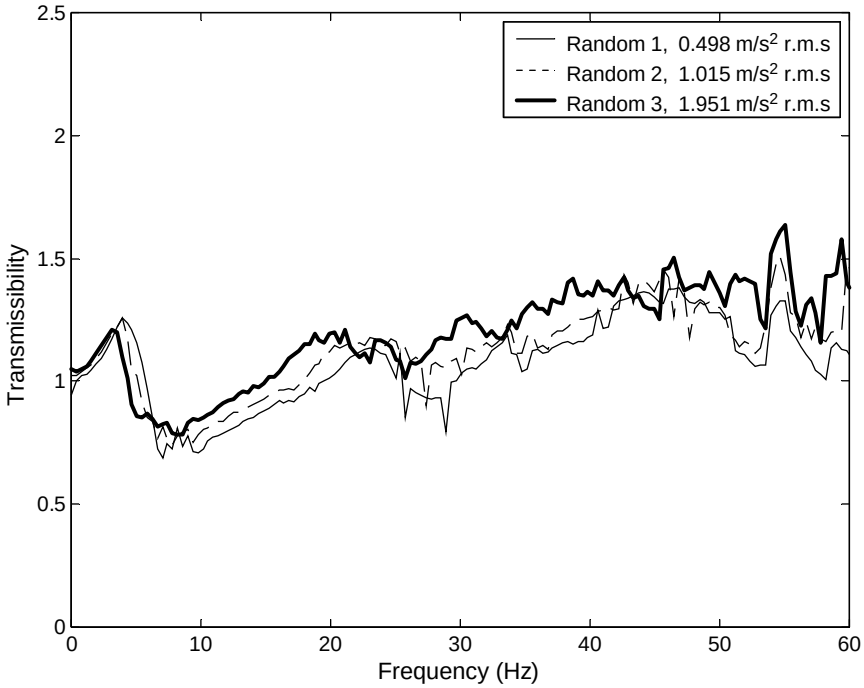


Fig. 16. Median transmissibility of the seat pan from 12 subjects and three random vibration inputs (acceleration r.m.s. values = 0.498, 1.015 and 1.951 $m\,s^{-2}$), laboratory simulation

transmissibility at all frequencies and not merely at the dominant frequencies in the vehicle vibration spectrum. Furthermore, it is possible to measure the transmissibility in each axis without resort to multiple coherency measurements and concern that motion in one axis on the seat is caused by motion in another axis at the seat base.

## 4. Conclusion

The road test showed that for fore–aft vibration, a single-input and single-output representation of seat transmissibility is insufficient. Fore–aft vibration on the seat and on the backrest was induced not only by fore–aft vibration on the floor but also by vertical floor vibration, partly due to the inclination of the seat and backrest. A study of a two-input and one-output model for fore–aft transmissibilities to both the backrest and the seat pan produced improved coherencies, showing that the determination of fore–aft seat transfer functions in a vehicle should recognize that the seat is a multiple-input and multiple-output system.

Measurements in the laboratory found three resonance frequencies in the transmissibility from the floor to the backrest in the fore–aft direction: one at about 5 Hz, another around 28 Hz and the third at about 48 Hz. The first two peaks appeared consistent with the road test results. For about 40% of subjects participating in the experiment, the backrest transmissibility only presented one resonance frequency (at about 5 Hz). The results showed that for the transmission of fore–aft

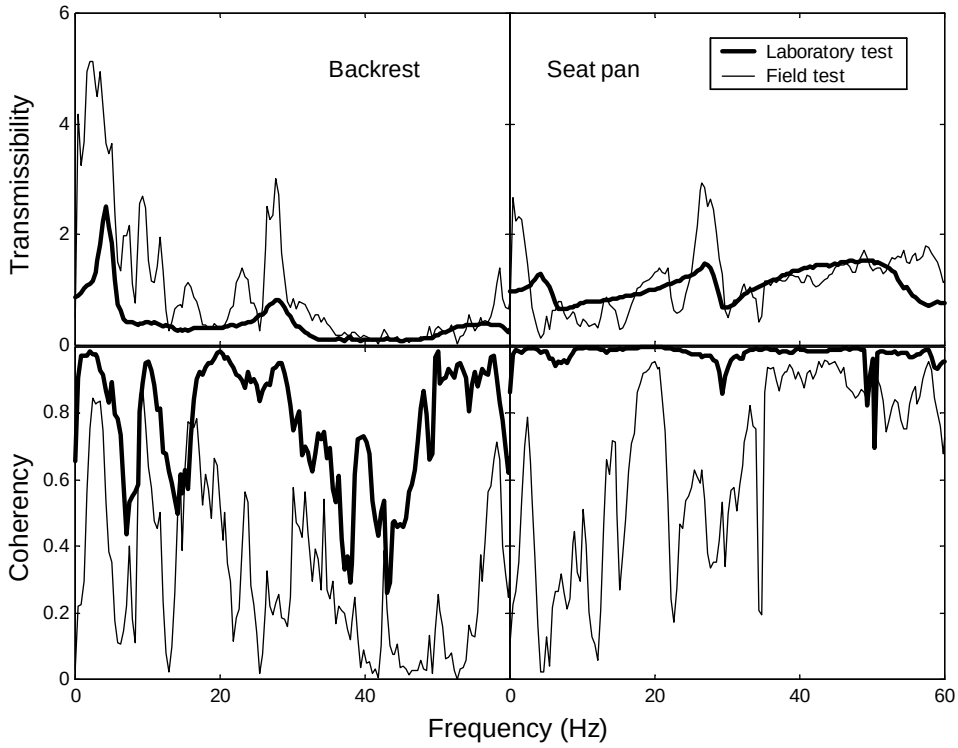


Fig. 17. Comparison of transmissibilities and coherencies from single-input and single-output model between the field test and the laboratory simulation (0.39 Hz resolution, 96 degrees of freedom).

vibration from the floor to the seat pan, the seat–person system presented three resonance frequencies in the range 0–60 Hz, with the most distinctive resonance located at about 5 Hz. Although the peaks are not as obvious as for the backrest, the three resonance frequencies were located at about the same frequencies. The coherency for fore–aft transmissibility to the seat pan was much higher than that to the backrest. The laboratory tests revealed that the seat–person system was non-linear at both the backrest and the seat pan. For the backrest–person system, the primary peak of the transmissibility decreased with increasing vibration magnitude, whereas for the second mode of vibration, the resonance frequency decreased with increasing vibration magnitude. For the seat pan–person system, at both the first and second modes of vibration, the resonance frequencies decreased with increasing vibration magnitude; the peak of the transmissibility at the first mode decreased with increasing magnitude, whereas at the second resonance and the frequencies above it, the transmissibility increased with increasing vibration magnitude.

Although the trends in the transmissibilities and resonance frequencies in the field test and the laboratory simulation were similar, there were differences between the two methods. The differences may have arisen for several reasons: (i) multiple inputs involved in the field test compared to the single input in the laboratory test; (ii) low-level inputs at some frequencies in the field test compared to well-defined inputs in the laboratory simulation and (iii) non-rigidity of

the seat base in the field test. Both laboratory and field methods have their advantages and disadvantages. A higher coherency can be obtained using the laboratory experimental method than when using the field test. With the field test, the correct vibration input spectra and the correct subject posture can be more easily used. It has been shown that the low coherency encountered in the field test with a single-input single-output model can be improved by adopting a two-input and one-output system model.

## Acknowledgements

This research was funded by the Ford Motor Company Ltd. The authors would like to acknowledge the support of Mr. Jon Willey, Mr. Martin Jansz and Dr. Stephen Jones.

## References

[1] C. Corbridge, M.J. Griffin, P. Harborough, Seat dynamics and passenger comfort, Institute of Mechanical Engineers Part F: Journal of Rail and Rapid Transit 203 (1989) 57–64.
[2] M.J. Griffin, The evaluation of vehicle vibration and seats, Applied Ergonomics 9.1 (1978) 15–21.
[3] T.E. Fairley, Predicting the Dynamic Performance of Seats, Ph.D. Thesis, University of Southampton, 1986.
[4] British Standards Institution, Guide to the measurement and evaluation of human exposure to whole-body mechanical vibration and repeated shock, British Standard, BSI 6841, 1987.
[5] International Organization for Standardization, Mechanical vibration and shock—evaluation of human exposure to whole-body vibration—Part I: general requirements, International Standard, ISO 2631-1, 1997.
[6] M.J. Griffin, Handbook of Human Vibration, Academic Press, London, 1996.
[7] Y. Qiu, Measurement of seat transmissibility for fore–aft vibration in a car, Proceedings of 36th UK Group Meeting on Human Response to Vibration, 12–19 September 2001, DERA, Farnborough, UK, 2001.
[8] J.S. Bendat, A.G. Piersol, Random Data Analysis and Measurement Procedures, 2nd Edition, Wiley, New York, 1986.
[9] S. Siegel, N.J. Castellan, Nonparametric Statistics for the Behavioural Sciences, 2nd Edition, McGraw-Hill, New York, 1988.